# Ultralarge Rydberg dimers in optical lattices

B. Vaucher,[*] S. J. Thwaite, and D. Jaksch

*Clarendon Laboratory, University of Oxford, Parks Road, Oxford, OX1 3PU, United Kingdom*

(Received 22 August 2008; published 20 October 2008)

We investigate the dynamics of Rydberg electrons excited from the ground state of ultracold atoms trapped in an optical lattice. We first consider a lattice comprising an array of double-well potentials, where each double well is occupied by two ultracold atoms. We demonstrate the existence of molecular states with equilibrium distances of the order of experimentally attainable interwell spacings and binding energies of the order of $10^3$ GHz. We also consider the situation whereby ground-state atoms trapped in an optical lattice are collectively excited to Rydberg levels, such that the charge-density distributions of neighboring atoms overlap. We compute the hopping rate and interaction matrix elements between highly excited electrons separated by distances comparable to typical lattice spacings. Such systems have tunable interaction parameters and a temperature $\sim 10^4$ times smaller than the Fermi temperature, making them potentially attractive for the study and simulation of strongly correlated electronic systems.

## I. INTRODUCTION

Recent advances in the trapping and manipulation of ultracold atomic gases have provided experimentalists with the ability to coherently control large numbers of atoms. Two areas that have become the focus of experimental efforts of late are the use of ultracold atoms for the formation and manipulation of molecules [1,2] and the creation and manipulation of Rydberg atoms in optical lattices [3]. In this paper we study whether a combination of these areas might lead to the production of diatomic molecules whose nuclear position is fixed by an optical lattice [see Figs. 1(a) and 1(b)]. In particular, we examine the properties of ultralarge dimers with equilibrium distances of the order of typical lattice spacings and binding energies of the order of $10^3$ GHz. We also investigate the prospect of using systems of interacting Rydberg atoms to simulate Fermi systems.

Molecules have a far richer energy structure than atoms, and can also have stronger long-range interactions, a feature that offers new possibilities for quantum control (see, e.g., [4]). However, the cooling of molecules is notably difficult, since the absence of closed electronic transitions prevents the use of standard laser cooling procedures. An attractive approach to producing translationally cold molecules is thus to form them from precooled atoms by way of photoassociation or magnetic resonance techniques. In recent years several classes of ultracold molecules have been predicted and produced, including Feshbach molecules, Efimov trimers, and the famous "trilobite" molecules, which are composed of a highly excited Rydberg atom interacting with another atom in its ground state [5,6]. The existence of long-range molecules composed of two Rydberg atoms stabilized via dipole-dipole interactions has also been predicted [7–9]. These ultracold long-range Rydberg molecules have binding energies of the order of several hundred megahertz (a factor of $\sim 10^6$ greater than the typical temperature of ultracold atoms, but

weak by molecular standards), a lifetime expected to be similar to that of Rydberg atoms, and equilibrium distances of the order of $10^4 a_0$ (with $a_0$ the Bohr radius) [8]. Recent advances in high-resolution microscopy techniques may offer new possibilities to study the spatial structure of such molecules [10]. Theoretical treatments of Rydberg molecules to date have primarily dealt with the regime in which the internuclear separation is greater than the Le Roy radius. In this regime the overlap between the atomic charge-density distributions is vanishingly small [7,8]. In contrast to these works, we consider the regime where the internuclear distance of the molecular dimer is comparable to typical lattice spacings, but smaller than the Le Roy radius, in which case the overlap of the charge distributions and effects such as the exchange interaction must be taken into account.
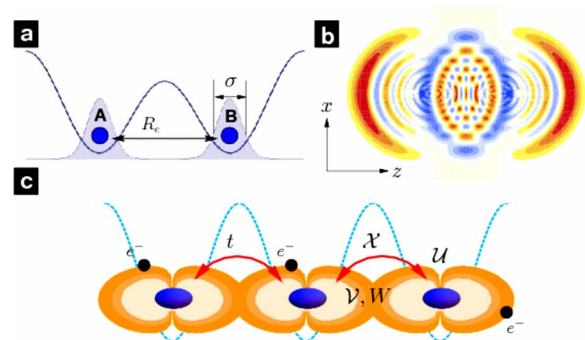


FIG. 1. (Color online) An optical lattice with pairs of atoms well separated from each other is initialized (a). A laser pulse transfers each pair of atoms to a molecular state with a very large internuclear distance. (b) Density plot of a typical diatomic molecular wave function on the $x$-$z$ plane ($y=0$) in the relative coordinates of two electrons in highly excited $np_z$ states. (c) The outer electron of each ground-state atom trapped in an optical lattice is transferred into a Rydberg state, such that the charge-density distributions between neighboring atoms overlap. The electron hopping rate $t$ becomes nonzero, and the interactions between electrons can be described by the parameters $\mathcal{U}$ (on-site interaction), $\mathcal{V}$, $\mathcal{W}$, and $\mathcal{X}$ (off-site interactions).

*benoit.vaucher@merton.ox.ac.uk; http://www.physics.ox.ac.uk/qubit

The simulation of condensed-matter systems is another area to which optical lattices are uniquely suited. Optical lattices have extremely flexible geometries, and by a suitable choice of laser configuration, any desired lattice structure can be created [11,12]. Fermions loaded into an optical lattice can be used as a model of electrons in a solid, with the significant advantage of having a periodic potential that is defectless and fully customizable [13]. However, the ratio between the currently attainable temperature $T$ of fermionic atoms trapped in an optical lattice and the Fermi temperature $T_F$ of the system is $T/T_F \sim 0.25$, preventing the clean observation of such interesting phenomena as the BCS transition or the emergence of certain types of antiferromagnetic order [13–15]. In the final section of this paper we consider the possibility of collectively transferring a population of ground-state atoms trapped in an optical lattice to a highly excited Rydberg level, such that the charge-density distributions of neighboring atoms overlap [see Fig. 1(c)]. We extend the model developed in the first section to compute the hopping rate and interaction parameters between the highly excited electrons, and determine the dependence of these quantities on the initial lattice spacing. While the implementation of these systems is experimentally challenging and beyond the scope of this paper [16], we note that experimental temperatures far smaller than the Fermi temperature ($T/T_F \sim 10^{-4}$) might be readily attainable, making the realisation of such systems a promising approach to the quantum simulation of interacting fermions.

The paper is organized as follows. In Sec. II we present the model that we subsequently use to investigate the existence of attractive molecular potentials with equilibrium distances below the Le Roy radius. We approximate the lifetime of these molecules and calculate their equilibrium internuclear distance for different values of the principal quantum number of the electrons. In Sec. III we use the model introduced in the first section to compute the hopping rate and interaction parameters of the Rydberg electrons and discuss the possibility of using these setups to simulate condensed-matter systems. We conclude in Sec. IV.

## II. MOLECULAR POTENTIALS OF ULTRALARGE RYDBERG DIMERS

In this section we present a method of evaluating the energy of highly excited diatomic molecular states whose equilibrium distance $R_e$ is below the Le Roy radius. We develop an efficient method of computing one- and two-center molecular integrals over electronic orbitals with large principal quantum numbers $n$ and calculate the depth and equilibrium position of molecular potentials accessible from the ground state via photoassociation for values of $n$ up to $n=35$. We estimate the radiative lifetime of the highly excited molecular potentials.

Quantum chemistry methods commonly used within the Le Roy radius typically become computationally expensive when dealing with Rydberg molecules due to the size of the basis set required to describe the spatially diffuse Rydberg orbitals. In order to obtain qualitative results in this computationally challenging regime we take a simple wave function ansatz inspired by the Heitler-London treatment of the hydrogen molecule. Due to the simplistic form of the molecular wave functions used we do not expect the method presented to produce quantitatively accurate results; rather, our aim is to obtain qualitatively correct results and insights within a regime where common methods of calculating molecular potentials fail or become computationally costly.

### A. Model

We consider an optical lattice potential forming an array of double wells separated from each other by sufficiently high optical barriers that each double well can be considered as an isolated system [17]. We assume that each double well initially contains two $^{87}$Rb atoms in their ground state, and that the potential is sufficiently deep that the Wannier function associated with each atom is well localized in one half of the well. Because alkali atoms have only a single valence electron, their energy levels are described by the same quantum numbers as those of the hydrogen atom. If the ground-state atoms are excited to Rydberg levels with $n > 30$ by applying a laser pulse to the system, the charge distributions of atoms in the same double well will overlap, and under certain conditions a stable molecular state will be formed. We aim to study the basic properties of these molecules and explore whether they may be produced in an optical lattice with experimentally realistic parameters. Since the temperature of the system is very low, the velocity of the electrons—even in highly excited states—is much greater than that of the trapped ions, and the electrons respond almost instantaneously to displacements of the ions [8]. Consequently, we will calculate molecular potentials in the Born-Oppenheimer (BO) approximation [18,19].

Neglecting interactions between atoms belonging to different double wells, the energy of a homonuclear molecule formed by the atoms in a double well is given within the BO approximation by the eigenvalues of the Hamiltonian

$$H(R) = -\frac{\hbar^2}{2m_e}(\nabla^2_{\mathbf{r}_1} + \nabla^2_{\mathbf{r}_2})$$
$$+ j_0\left(\frac{1}{R} + \frac{1}{r_{12}} - \frac{1}{r_{1A}} - \frac{1}{r_{1B}} - \frac{1}{r_{2A}} - \frac{1}{r_{2B}}\right), \quad (1)$$

where $\mathbf{r}_i$ ($i=1,2$) is the position of the $i$th electron; $r_{i\xi}$ ($\xi =A,B$) is the distance between the $i$th electron and atomic center $\xi$; $r_{12}$ is the distance between the two electrons; $j_0 = e^2/(4\pi\varepsilon_0)$, where $\varepsilon_0$ is the permittivity of free space and $e$ the elementary unit of charge; and $R$ is the distance between the nuclei. In the BO approximation $R$ is treated as a classical variable upon which the eigenvalues and eigenfunctions of the Hamiltonian depend parametrically. Following a similar approach to that of Ref. [9,20], we approximate the energy of the molecule by diagonalizing the Hamiltonian (1) using as a basis the asymptotic electronic states

$$\Psi^{\pm}_{\mathbf{q},\mathbf{q}'} = \mathcal{N}^{\pm}_{\mathbf{q},\mathbf{q}'}[A_{\mathbf{q}}(\mathbf{r}_1)B_{\mathbf{q}'}(\mathbf{r}_2) \pm A_{\mathbf{q}}(\mathbf{r}_2)B_{\mathbf{q}'}(\mathbf{r}_1)], \quad (2)$$

where $A_{\mathbf{p}}(\mathbf{r}_i)$ [$B_{\mathbf{p}}(\mathbf{r}_i)$] is a hydrogen-like wave function with quantum numbers $\mathbf{q}=(n,\ell,m)$ centered on nucleus $A$ ($B$), and $\mathcal{N}^{\pm}_{\mathbf{q},\mathbf{q}'}=[2(1 \pm |S_{\mathbf{q},\mathbf{q}'}|^2)]^{-1/2}$ is a normalization factor,

where $S_{\mathbf{q},\mathbf{q}'} = \int d\mathbf{r} A_{\mathbf{q}}^*(\mathbf{r}) B_{\mathbf{q}'}(\mathbf{r})$ is the overlap integral [18]. The basis elements that are symmetric or antisymmetric in the coordinates have an associated antisymmetric (singlet) or symmetric (triplet) function of spins, respectively. Each basis state (2) describes the two electrons being exchanged between the two nuclei, and corresponds to an ansatz for a valence-bond wave function [19]. The diagonal elements of the Hamiltonian (1) using the states (2) as a basis correspond to the molecular potentials obtained using the Heitler-London method [18,21].

The hydrogenic wave function of the valence electron centered on atom $\xi$ located at $\mathbf{r}_\xi$ is well approximated by the (unnormalized) function

$$\xi_{\mathbf{q}}(\mathbf{r}) = P_\ell(\cos\theta_\xi) \frac{e^{im\phi}}{a_0^{3/2}} \left(\frac{2\rho_\xi}{n^*}\right)^{n^*} e^{-\rho_\xi/n^*} \sum_{k=0}^{k_{\max}} b_k \rho_\xi^{-(k+1)}. \quad (3)$$

Here $\rho_\xi = r_\xi/a_0$ with $r_\xi = |\mathbf{r} - \mathbf{r}_\xi|$ the radial distance from the atomic center $\xi$, $\theta_\xi$ is the angle between the vector $\mathbf{r}_\xi$ and the internuclear axis, $\phi$ is the azimuthal angle, $P_\ell(x)$ is a Legendre polynomial, and $n^* = n - \delta_\ell$ is the effective principal quantum number, with $\delta_\ell$ a quantum defect whose value depends on the angular momentum quantum number $\ell$ and the atomic species [22]. The coefficients $b_k = b_{k-1}(n^*/2k)[\ell(\ell+1) - (n^*-k)(n^*-k+1)]$ are defined recursively with $b_0 = 1$, and $k_{\max}$ is an integer satisfying $n^* - \ell - 1 \leq k_{\max} < n^* - \ell$ [23,24]. The orbital defined in Eq. (3) is known as the asymptotic form of the quantum defect wave function; for $\delta_\ell = 0$, it is identical to the hydrogenic wave function, while for $\delta_\ell \neq 0$ it provides an accurate description of a Rydberg electron in the mid- and long-range. It differs significantly from the exact quantum defect wave function only at short distances from the atomic cores, which is of little consequence since the interactions we consider here depend mainly on the outer part of the atomic wave functions.

For $n > 20$, the overlap between the charge-density distributions of atoms separated by distances smaller than the Le Roy radius (for $\mathbf{q} = \mathbf{q}'$) is typically of the order of $S_{\mathbf{q},\mathbf{q}'} \sim 10^{-1} - 10^{-2}$. The charge-density overlap is therefore not negligible in this regime, and the approximation of the Coulomb potential using the multipole expansion [25,26] is not suitable. The multipole expansion diverges quite significantly from the Coulomb potential even in the presence of small charge-density overlap, and so the results obtained using this approximation below the Le Roy radius are very uncertain [8,27].

We consequently estimate the energy of the dimer by evaluating the expectation value of the Hamiltonian (1) in the states (2), a task that requires the evaluation of a number of integrals over atomic orbitals. These integrals fall into two classes: the *one-center* integrals, comprising the overlap integral $S_{\mathbf{q},\mathbf{q}'}$, the Coulomb integral $J_{\mathbf{q},\mathbf{q}'}$ $= j_0 \int d\mathbf{r} B_{\mathbf{q}}^*(\mathbf{r})(1/r_A) B_{\mathbf{q}'}(\mathbf{r}) = j_0 \int d\mathbf{r} A_{\mathbf{q}}^*(\mathbf{r})(1/r_B) A_{\mathbf{q}'}(\mathbf{r})$, and the charge overlap integral $K_{\mathbf{q},\mathbf{q}'}^\xi = j_0 \int d\mathbf{r} A_{\mathbf{q}}^*(\mathbf{r})(1/r_\xi) B_{\mathbf{q}'}(\mathbf{r})$; and the *two-center* integrals

$$U_{\mathbf{p},\mathbf{p}'}^{\mathbf{q},\mathbf{q}'} = [A_{\mathbf{q}} A_{\mathbf{q}'} | A_{\mathbf{p}} A_{\mathbf{p}'}], \quad W_{\mathbf{p},\mathbf{p}'}^{\mathbf{q},\mathbf{q}'} = [A_{\mathbf{q}} B_{\mathbf{q}'} | A_{\mathbf{p}} B_{\mathbf{p}'}], \quad (4)$$

TABLE I. Replacement rules used to generate analytical formulas for one-center integrals; $\Gamma_k(x)$ is the incomplete gamma function with $k \in \mathbb{N}_+$.

| Rule | Functional | Replacement |
|---|---|---|
| $R1$ | $\int_1^\infty dx\, e^{-\alpha x} x^k \rightarrow (1/\alpha^{1+k})\Gamma_{1+k}(\alpha)$ | |
| $R2$ | $\int_{-1}^1 dx\, e^{\beta x} x^k \rightarrow [(-\beta)^{-k}/\beta][\Gamma_{1+k}(-\beta) - \Gamma_{1+k}(\beta)]$ | |

$$V_{\mathbf{p},\mathbf{p}'}^{\mathbf{q},\mathbf{q}'} = [A_{\mathbf{q}} A_{\mathbf{q}'} | B_{\mathbf{p}} B_{\mathbf{p}'}], \quad X_{\mathbf{p},\mathbf{p}'}^{\mathbf{q},\mathbf{q}'} = [A_{\mathbf{q}} A_{\mathbf{q}'} | A_{\mathbf{p}} B_{\mathbf{p}'}], \quad (5)$$

where

$$[\alpha\beta|\gamma\nu] = j_0 \int\int d\mathbf{r}_1 d\mathbf{r}_2 \alpha^*(\mathbf{r}_1)\beta(\mathbf{r}_1) \frac{1}{r_{12}} \gamma^*(\mathbf{r}_2)\nu(\mathbf{r}_2). \quad (6)$$

The evaluation of one- and two-center molecular integrals poses a considerable challenge for large values of the principal quantum numbers. The results of such integrals using direct numerical integration converge extremely slowly, and the answers so produced can suffer from dramatic losses of accuracy (a phenomenon known as numerical erosion; see, e.g., [28,29]). Following an approach suggested by Barnett, we use a computer algebra-based method to generate analytical formulas for the molecular integrals [28,30,31]. We have found this approach advantageous for three reasons: (i) it permits the fast evaluation of molecular integrals with high principal quantum number to arbitrary accuracy; (ii) once the analytical form has been found, the evaluation of an integral for different values of the internuclear distance is instantaneous; (iii) the analytical expressions of the integrals can be stored and reused at little computational cost.

However, even with the use of symbolic calculations, the evaluation of molecular integrals for large values of $n$ is computationally demanding. In order to make these calculations tractable for large $n$ we restrict the value of the projection of the electronic angular momentum along the internuclear axis to $m = 0$. This limits the range of molecular states that can be investigated to those of symmetry $^1\Sigma_g^+$ and $^3\Sigma_u^+$; these are associated with the $\Psi_{\mathbf{q},\mathbf{q}'}^+$ and $\Psi_{\mathbf{q},\mathbf{q}'}^-$ basis states, respectively. In this way we have been able to compute molecular integrals involving wave functions with principal quantum numbers up to $n = 35$.

In order to compute the molecular integrals it is convenient to express the electron coordinates in elliptical coordinates $(\lambda, \mu, \phi)$ through the relations $r_\xi = (R/2)(\lambda \pm \mu)$ and $\cos\theta_\xi = [(1 \pm \lambda\mu)/(\lambda \pm \mu)]$, where plus and minus signs apply to $\xi = A$ and $\xi = B$, respectively. The volume element is given by $d\mathbf{r} = (R/2) r_A r_B d\lambda\, d\mu\, d\phi$, where $0 \leq \phi \leq 2\pi$, $-1 \leq \mu \leq 1$, and $1 \leq \lambda \leq \infty$. After rounding up the powers of $r_\xi$ in Eq. (3) to the next integer value (which significantly affects the shape of the wave function only near the core) we find that the integrands of all of the one-center integrals can be written in the form $e^{-\alpha\lambda} e^{\beta\mu} \Sigma_{ij} q_{i,j} \lambda^i \mu^j$ where $q_{i,j}$ are coefficients associated with a given integral. By applying the replacement rules defined in Table I, every one-center integral can be converted into an analytical expression with parametric dependence on $R$.
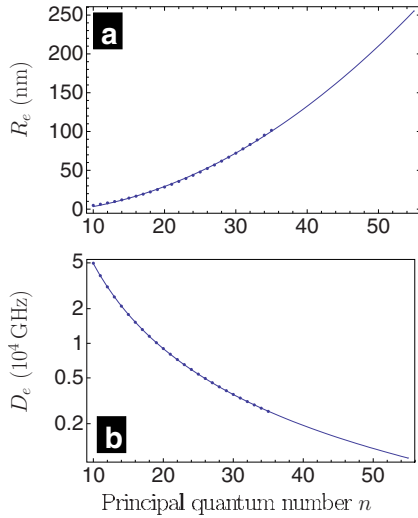
FIG. 2. (Color online) Equilibrium distance $R_e$ (a) and potential depth $D_e$ (b) of the $np+np$ states using the Heitler-London method. The dots denote the values calculated numerically, while the curves correspond to the fitted functions mentioned in the text.

The evaluation of symbolic expressions for two-center integrals proceeds similarly, although many more replacement rules are required. The general approach for two-center integrals consists of expressing the Coulomb potential in the form of a sum of polynomials (such as the Legendre or Neumann expansion) before applying replacement rules on the terms resulting from the successive integrations over the coordinates of the first and second valence electron. Using this method, exact formulas are obtained for Eqs. (4), but only approximate expressions may be found for Eqs. (5) (see the Appendix).

### B. Results

Since we envisage producing the Rydberg dimers by applying a laser pulse to a system of ground-state atoms, we are primarily interested in the molecular states that are most strongly coupled to ground-state atoms by the dipole transition operator; namely, those of $^3\Sigma_u^+$ symmetry with a high $p$-character ($\ell=1$). We will therefore restrict our analysis to these states. However, for values of $n \geq 10$ molecular states of $^3\Sigma_u^+$ and $^1\Sigma_g^+$ symmetry become quasidegenerate [8,26], and so the results presented here apply to molecular states of either of these symmetries.

We have estimated the equilibrium distances $R_e$ and potential depths $D_e = E_{mol}(\infty) - E_{mol}(R_e)$ of $np+np$ molecular potentials of $^3\Sigma_u^+$ symmetry using the Heitler-London approach for values of the principal quantum number up to $n=35$ (see Fig. 2). We find that the equilibrium distance of these potentials follows the relation $R_e \simeq (1.628n^2 - 100.25)a_0$, which is about a factor of 4 smaller than the Le Roy radius for all values of $n$ [see Fig. 2(a)]. For larger values of the principal quantum number ($n>35$), we find that the equilibrium distances predicted by our scaling law are comparable to (although ~20% smaller than) those found by Boisseau *et al.* in Ref. [8], who use the multipole
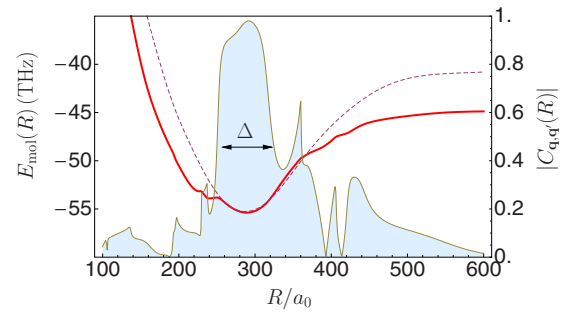


FIG. 3. (Color online) Left axis: $^3\Sigma_u$ molecular potential (solid red line) associated with the wave function $\Psi_{mol}(R)$ resulting from the diagonalization of the Hamiltonian (see text) for $n=16$. The dashed line shows the molecular potential for the $np+(n-1)p$ bare state. Right axis: Contribution $C_{\mathbf{q},\mathbf{q}'}(R)$ of the $\mathbf{q}=(16,1,0)$, $\mathbf{q}'=(15,1,0)$ basis state to the molecular wave function $\Psi_{mol}(R)$; $\Delta$ denotes the width of the region over which this contribution is dominant.

expansion of the Coulomb potential to examine the same potentials below the Le Roy radius.

The depth of the molecular potential for $n=35$ is $D_e \simeq 2000$ GHz, approximately three orders of magnitude larger than the potential depth of ultralarge molecules with symmetry $^1\Pi_g-^3\Pi_u$ bonded via dipole-dipole interactions studied in Ref. [8] [see Fig. 2(b)]. We find that the molecular binding energy decreases exponentially with the value of the principal quantum number according to the relation $D_e = \exp(\alpha_1 + \alpha_2 n^{\beta_2} + \alpha_3 n^{\beta_3})$ GHz where $\alpha_1 = -6.53$, $\alpha_2 = -24.44$, $\alpha_3 = -20.51$, $\beta_2 = 0.14$, and $\beta_3 = -223.45$. Our predicted potential depths differ by up to an order of magnitude from those calculated using the multipole expansion; as Boisseau *et al.* point out in Ref. [8], this is probably a consequence of the inaccuracy of the multipole expansion below the Le Roy radius. Although the potentials produced using our method do not have the asymptotic $R^{-5}$ behavior expected from perturbation theory [26], this may be corrected by carrying out a numerical integration of the terms which were neglected during the symbolical calculations of the molecular integrals. This correction is feasible for small values of $n$, but very time consuming for larger values. However, a comparison with the results of exact numerical calculations of the same potentials up to $n=8$ shows that our method reproduces the correct values of $R_e$ and $D_e$ within ~3%.

Following the approach taken in Ref. [9], we diagonalized the Hamiltonian using as a basis the molecular states (2) with a significant coupling to the $np+n'p$ asymptote. For $n'=n-1$ and $n=16$ we used the states $(n-1)s+(n+1)s$, $(n-1)s+ns$, $(n-1)s+(n+2-k)d$, $(n-2)d+(n-k)d$, $(n-3)d+(n-k+1)d$, and $(n-1-k')p+(n+k)p$, with $k,k'=1,2$. The diagonalization procedure yields eigenstates of the form $\Psi_{mol}(R) = \Sigma C_{\mathbf{q},\mathbf{q}'}(R)\Psi_{\mathbf{q},\mathbf{q}'}$, allowing the determination of the contribution of a given molecular state $\Psi_{\mathbf{q},\mathbf{q}'}$ to each eigenstate. Figure 3 shows the contribution of the asymptotic $np+(n-1)p$ state to an eigenstate $\Psi_{mol}$, and the potential curve $E_{mol}(R)$ corresponding to this eigenstate, for the case of $n=16$. In a region of width $\Delta$ about $R_e$ the molecular potential is indistinguishable from that of the bare $np+n'p$ state, and the associated wave function has a very dominant $np+n'p$

character [$C_{\mathbf{q},\mathbf{q}'}=0.98$ with $\mathbf{q}=(16,1,0)$ and $\mathbf{q}'=(15,1,0)$; see Fig. 3]. This is due to the fact that the coupling between different states is generally weak (off-diagonal elements of the Hamiltonian are typically $\sim 10^{-1}-10^{-3}$ smaller than diagonal ones) and the strongest coupling is seen between states with identical angular momentum.

We find that the size of the region $\Delta \simeq 0.24 n^2 a_0$ is approximately a factor of 3 smaller than the width of the molecular potential associated with the bare $np+(n-1)p$ states (approximately given by $0.73 n^2 a_0$). This provides an indication of the nature of the wave function of the molecular states accessible by the photoassociation of ground-state atoms initially trapped in an optical lattice. The distance $a_{\mathrm{dw}}$ between the two sides of a double well may be controlled by altering the laser parameters. The uncertainty in the initial position of the ground-state atoms is given by the width of their Wannier functions (see Fig. 1), which is proportional to $\sigma = a_{\mathrm{dw}}/[\pi(\widetilde{V}/E_R)^{1/4}]$, where $\widetilde{V}$ is the depth of the double well and $E_R$ the recoil energy [32]. By setting $a_{\mathrm{dw}}=R_e$ and considering the scaling of the width of the $np+(n-1)p$ molecular potentials, we find that $2\sigma \lesssim \Delta$ for lattice potential depths of the order of $\widetilde{V}=(30-40)E_R$. This suggests that using an optical lattice to enforce the initial position of the atoms before applying the photoassociation pulse might offer advantages in providing access to molecular states with a very dominant $np+n'p$ character.

We have obtained an order-of-magnitude estimate of the lifetime of the photoassociated molecules by assuming for simplicity that the dominant decay mode is radiative dissociation into a pair of $^{87}$Rb atoms. We neglect the rotational fine structure of the energy levels and any bound-bound decay channels and consider a transition between a bound state of vibrational quantum number $\nu'$ and energy $E_{\nu'}$ and a free continuum state of wave number $k''$ and energy $E_{k''}=\hbar^2 k''^2/(2\mu)$, where $\mu=m_{\mathrm{Rb}}/2$ is the reduced mass of the molecule. The Einstein $A$ coefficient is given by

$$A_{\nu'k''}=\frac{32\pi^3}{3\varepsilon_0 h^5 c^3}\sqrt{\frac{2\mu}{E_{k''}}}(E_{\nu'}-E_{k''})^3$$
$$\times \left|\int [\psi_{\nu'}^{\mathrm{vib}}(R)]^* D(R)\psi_{k''}^{\mathrm{vib}}(R)dR\right|^2 J^{-1} s^{-1}, \quad (7)$$

while the radiative lifetime of a single bound vibrational level is given by $\tau_{\nu'}=A_{\nu'}^{-1}$, where

$$A_{\nu'}=\int_0^\infty A_{\nu'k''}dE_{k''}. \quad (8)$$

Here $h=2\pi\hbar$ is the Planck constant, $c$ is the speed of light, $\psi_{\nu'}^{\mathrm{vib}}$ and $\psi_{k''}^{\mathrm{vib}}$ are vibrational wave functions for the discrete and continuum states, respectively, and the dipole moment $D(R)$ is given by

$$D(R)=-e\int\int d\mathbf{r}_1 d\mathbf{r}_2 [\Psi_{\mathbf{q}_i,\mathbf{q}_i}^{\pm}]^*(z_1+z_2)\Psi_{\mathbf{q}_f,\mathbf{q}_f}^{\pm}, \quad (9)$$

where $z_1$ and $z_2$ are the $z$ coordinates of the electrons and $\mathbf{q}_i$ and $\mathbf{q}_f$ denote the quantum numbers of the initial and final
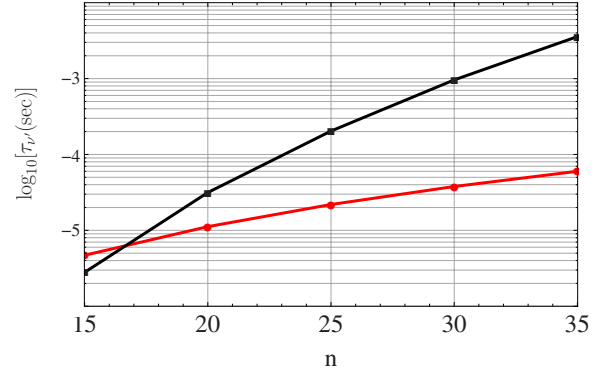


FIG. 4. (Color online) Radiative lifetimes for the $\nu'=0$ vibrational level in molecular excited states with principal quantum numbers $n=15-35$ (black line). The radiative lifetime $\tau=\tau_0 n^3$ of a free Rydberg atom is plotted for comparison purposes [red (gray) line].

states. For large internuclear distances the continuum wave function $\psi_{k''}^{\mathrm{vib}}$ has the asymptotic form

$$\psi_{k''}^{\mathrm{vib}}\sim \sin(k''R+\eta), \quad (10)$$

where $\eta$ is the scattering phase shift, which at low energies is given by $\eta=-k''a_s$ with $a_s$ the $s$-wave scattering length. In the initial molecular state we approximate the true bound vibrational wave functions $\psi_{\nu'}^{\mathrm{vib}}(R)$ by the eigenstates of a harmonic approximation to the molecular potential centered about $R=R_e$. Due to the asymmetric nature of the molecular potential curves, this approximation becomes progressively worse as $\nu'$ increases. However, we expect that the ability to impose an interatomic spacing close to the equilibrium distance of the targeted molecular state before applying the photoassociation pulse will provide a measure of control over the range of vibrational levels occupied by the molecules, thus making the lowest vibrational levels the most relevant.

Although there are a huge number of final states to which the molecule could decay, the dependence of the decay rate given by Eq. (7) on $(E_{\nu'}-E_{k''})^3$ favors transitions that involve the emission of a high-energy photon. We therefore consider only transitions that finish within the continuum above the $5s$-$5s$ potential curve, neglecting all other decay channels. The radiative lifetimes thus calculated for the ground vibrational state $\nu'=0$ are shown in Fig. 4; the lifetimes of higher vibrational levels (up to $\nu'=10$) are the same to within $\sim 5\%$. Also plotted for comparison purposes is the radiative lifetime $\tau=\tau_0 n^3$ of a free Rydberg atom, where $\tau_0=1.4$ ns for $^{87}$Rb [33]. Our calculations indicate that for $n\gtrsim 17$ the Rydberg dimers are more stable than the free atoms. For the highest molecular state considered ($n=35$) we find lifetimes of the order of a few milliseconds, indicating that, even if contributions from neglected decay channels were to reduce this lifetime by several orders of magnitude, the system could still be successfully interrogated and characterised by short (nanosecond to picosecond) laser pulses. To avoid possible stimulated emission contributions to the radiative decay process, the laser fields forming the optical lattice could be switched off as the Rydberg excitation pulse is applied. The subsequent free expansion of the atoms would not limit the

window of time within which the system may be characterized, since the atoms are expected to remain localized within a few lattice spacings for a time of the order of 10 $\mu$s [34].

## III. INTERACTIONS BETWEEN HIGHLY EXCITED ELECTRONS IN A LATTICE

In this section we consider the situation where ground-state atoms trapped in a regular optical lattice are collectively excited to a given Rydberg state such that the charge-density distributions of neighboring atoms overlap. With overlapping charge-density distributions between neighboring atoms, the valence electrons will tunnel between lattice sites and interact with each other, mimicking the behavior of electrons in metals. Such a system may have interesting applications for the quantum simulation of electrons in lattice systems. Assuming that the band structure of such a system is well described by a tight-binding model, we will find that using the hopping rate calculated in the next section that the Fermi temperature of a half-filled lattice is $T_F \sim 10^{-3}$ K, some five orders of magnitude larger than typical temperatures achieved in experiments with ultracold atoms. While the efficient population transfer of atoms to Rydberg states is experimentally very challenging and goes beyond the scope of this paper (see, e.g., Ref. [16]), this figure implies that after the excitation step, the system temperature could still remain well within the Fermi degeneracy regime ($T \ll T_F$). This would enable the observation of interesting many-body phenomena currently inaccessible to other experimental setups involving fermionic atoms where the ratio $T/T_F \approx 0.25$ (see, e.g., Refs. [13,35]). In this section, we use the tools developed previously to evaluate the typical interaction parameters and the hopping rate of such a system, and investigate their dependence on the interatomic spacing fixed by the lattice.

### Model

In this section we assume that ground-state atoms trapped in an optical lattice can be collectively excited to a given Rydberg state. We assume that the dynamics of the valence electrons in the lattice is restricted to only one spatial mode per site $i$ that corresponds to an orbital $\phi_i(\mathbf{r}) = \langle \mathbf{r} | \phi_i \rangle$ associated with a given Rydberg state localized at site $i$ with two spin orientation. The Hamiltonian of the system is then given by

$$\hat{H} = -\sum_{i,j,\sigma} t_{ij} \hat{c}_{i\sigma}^\dagger \hat{c}_{j\sigma} + \frac{1}{2} \sum_{\substack{i,j,k,l \\ \sigma,\sigma'}} V(i,j,k,l) \hat{c}_{i,\sigma}^\dagger \hat{c}_{j,\sigma'}^\dagger \hat{c}_{k,\sigma'} \hat{c}_{l,\sigma},$$

(11)

where $\hat{c}_{i\sigma}^\dagger$ is a creation operator associated with the orbital $\phi_i(\mathbf{r})$ and spin $\sigma$, $t_{ij}$ describes the hopping of a particles between sites $i$ and $j$; and the intersite interactions are given by

$$V(i,j,k,l) = \int \int dr \, dr' \, \phi_i^*(r) \phi_j^*(r') V_{ee}(r-r') \phi_k(r) \phi_l(r'),$$

(12)

where $V_{ee}(r-r')$ is the interelectronic potential. We assume here that next-nearest-neighbor hopping can be neglected, and consider only nearest-neighbor interactions. In this situation the hopping term $t = t_{i,i+1}$ consists of the kinetic energy and Coulomb potential of neighboring ion cores

$$t = \left\langle \phi_i \left| \left( -\frac{\hbar^2}{2M} \nabla^2 - \frac{j_0}{|\mathbf{r} - \mathbf{R}_i|} - \frac{j_0}{|\mathbf{r} - \mathbf{R}_{i+1}|} \right) \right| \phi_{i+1} \right\rangle, \quad (13)$$

and the only two-electron interaction terms taken into account are $\mathcal{U} = V(i,i,i,i)$, $\mathcal{X} = V(i+1,i,i,i)$, $\mathcal{V} = V(i,i+1,i+1,i)$, and $\mathcal{W} = V(i,i+1,i,i+1)$ [36].

Electronic orbitals centered at different lattice sites are often considered to be orthogonal and equated to the Wannier functions of the crystal [37]. However, a better definition of the Wannier function centered at site $i$ in terms of electronic orbitals is given by

$$\phi_i = \psi_i - \frac{S_i \psi_{i+1} + S_{i-1} \psi_{i-1}}{2}, \quad (14)$$

where $\psi_i$ is a normalized electronic wave function with quantum numbers centered at site $i$, and $S_i$ is the overlap between the orbitals of site $i$ and $i+1$ [38]. In the regime where the terms proportional to $S_i^2$ can be neglected, the functions $\phi_i$ form an orthonormal basis set. By inserting the definition (14) into Eqs. (12) and (13) and assuming that the site orbitals $\psi_i = \Psi_{\mathbf{q}}(\mathbf{r} - \mathbf{R}_i)$ correspond to hydrogenic wave functions with quantum numbers $\mathbf{q}$, the parameters of the Hamiltonian (11) can be expressed in terms of two-center molecular integrals as

$$\mathcal{U} = U_{\mathbf{q},\mathbf{q}}^{\mathbf{q},\mathbf{q}} - 4S_{\mathbf{q},\mathbf{q}} X_{\mathbf{q},\mathbf{q}}^{\mathbf{q},\mathbf{q}},$$

$$t = (E_{\mathbf{q}} + j_0/R) S_{\mathbf{q},\mathbf{q}} - 2K_{\mathbf{q},\mathbf{q}},$$

$$\mathcal{V} = V_{\mathbf{q},\mathbf{q}}^{\mathbf{q},\mathbf{q}} - 2S_{\mathbf{q},\mathbf{q}} X_{\mathbf{q},\mathbf{q}}^{\mathbf{q},\mathbf{q}}, \mathcal{W} = W_{\mathbf{q},\mathbf{q}}^{\mathbf{q},\mathbf{q}} - 2S_{\mathbf{q},\mathbf{q}} X_{\mathbf{q},\mathbf{q}}^{\mathbf{q},\mathbf{q}},$$

$$\mathcal{X} = X_{\mathbf{q},\mathbf{q}}^{\mathbf{q},\mathbf{q}} - S_{\mathbf{q},\mathbf{q}} \left( W_{\mathbf{q},\mathbf{q}}^{\mathbf{q},\mathbf{q}} + \frac{1}{2} (U_{\mathbf{q},\mathbf{q}}^{\mathbf{q},\mathbf{q}} + V_{\mathbf{q},\mathbf{q}}^{\mathbf{q},\mathbf{q}}) \right), \quad (15)$$

where $K_{\mathbf{q},\mathbf{q}} = K_{\mathbf{q},\mathbf{q}}^A = K_{\mathbf{q},\mathbf{q}}^B$, $\mathcal{U}$ is the on-site interaction, $\mathcal{V}$ and $\mathcal{W}$ are off-diagonal repulsion terms, and $\mathcal{X}$ is sometimes called the density-dependent hopping or enhanced hopping rate [39]. The absolute values of the ratios between different interaction parameters for atoms in $np_z$, $ns$, and $nd_{z^2}$ states ($n = 30$) are shown in Fig. 5, where we have plotted the parameters in Eq. (15) obtained with $S_i = 0$, that is, with Wannier functions represented by bare atomic orbitals. The orthogonalization procedure (i.e. replacing $\psi_i$ by $\phi_i$) mainly affects the smallest parameters $\mathcal{X}$ and $\mathcal{W}$ in the regions where the value of $S_i^2$ is not small enough for the Wannier functions to be effectively orthogonal.

The interaction parameters calculated above correspond to the intermediate screening case, that is $\mathcal{U} > \mathcal{V} \gg \mathcal{W}$ and $\mathcal{X} \simeq \kappa \mathcal{J}$, where $\kappa$ is a constant [40,41]. The ratios between the parameters are similar to those found in realistic systems, e.g., between $p$ electrons in conjugated polymers [40]. For different values of the angular momentum, these ratios differ mainly in the way they behave at large distances. The hop-
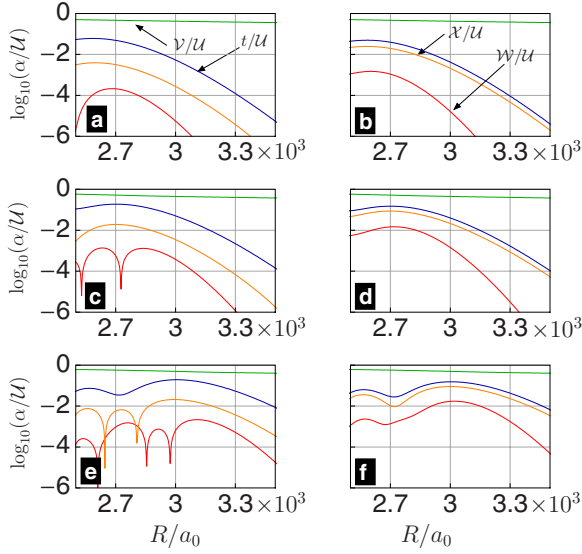
FIG. 5. (Color online) Relative values of the interaction parameters $(\alpha = \mathcal{V}, t, \mathcal{X}, \mathcal{W})$ of a Hubbard model of Rydberg electrons in a state with quantum numbers $\mathbf{q} = (30, \ell, 0)$. (a) $\ell = 0$ (b) $\ell = 0$, setting $S_{\mathbf{q},\mathbf{q}} = 0$; (c) $\ell = 1$ (d) $\ell = 1$, setting $S_{\mathbf{q},\mathbf{q}} = 0$; (e) $\ell = 2$ (f) $\ell = 2$, setting $S_{\mathbf{q},\mathbf{q}} = 0$. From top to bottom we have $\mathcal{V}/\mathcal{U}$ (green), $t/\mathcal{U}$ (blue), $\mathcal{X}/\mathcal{U}$ (orange), and $\mathcal{W}/\mathcal{U}$ (red).

ping rates $t$ are shown in Fig. 6, and, for the quantum numbers considered, vary between $10^2$ and $10^{-4}$ GHz for intersite distances between 150 and 250 nm, respectively.

## IV. CONCLUSION

We showed that optical lattices forming arrays of double-well potentials may be exploited to selectively photoassociate pairs of atoms to molecular states with binding energies of the order of $10^3$ GHz, far larger than those of long-range molecules stabilized by dipole-dipole forces. These molecular states are expected to have equilibrium distances of the order of the typical lattice spacings and lifetimes several orders of magnitude larger than the time scales required to interrogate and characterize them by way of short laser pulses.

We considered the possibility of collectively exciting ground-state atoms trapped in a regular lattice to a given
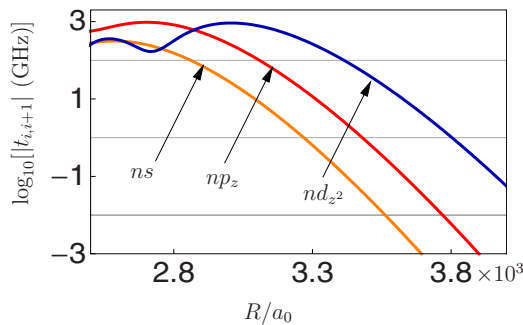


FIG. 6. (Color online) Hopping rate in the $z$ direction between sites separated by a distance $R$ for electrons in $ns$, $np_z$, and $nd_{z^2}$ states ($n = 30$).

Rydberg level such that the charge-density distributions of atoms located in neighboring sites overlap. Assuming that such a system could be realized, we calculated the typical interaction parameters between the Rydberg electrons and the hopping rate between sites. With a temperature well below the Fermi temperature and tunable interaction parameters, such systems might offer an interesting alternative approach to the simulation of Fermi systems. For instance, the ability to change the lattice spacing such that $v = \mathcal{U}/\mathcal{V} > \frac{1}{2}$ or $v < \frac{1}{2}$ would offer the possibility of engineering a charge-density wave (CDW) or a spin-density wave (SDW), respectively. The preparation of a SDW state could even be facilitated by using spin-changing collisions between ultracold $^{87}$Rb ground-state atoms to produce a Néel-like state $|\uparrow\downarrow\uparrow\downarrow\ldots\rangle$ that has a spin arrangement identical to that of the SDW ground state along one spatial direction [42]. If realized, such a system would allow the observation of a phase transition between the SDW and CDW phases, by, for example, the measurement of the zero-frequency SDW susceptibility[1] or the CDW structure factor, both of which diverge linearly in their respective phases [43]. Further, the versatility of optical lattice setups may allow the excitation of Rydberg atoms with a given angular momentum, which potentially enables exotic quantum phase transitions to be engineered: indeed, the value of the electronic angular momentum not only influences the relative values of the system interaction parameters, but also in some cases their signs (see, e.g., Refs. [44–46]). This feature is particularly interesting, as it is the mechanism behind e.g., the emergence of nontrivial and rich phase diagrams in doped cuprates (see, e.g., Refs. [47,48]). Finally, if in addition the electron density could be controlled when producing one of these states, it would provide the exciting possibility of turning the state of the electrons into a superconductor, as happens in the case of doping-induced superconductivity in cuprates [49]. The parameters calculated in this work apply to models where the dynamics of the electrons is restricted to one mode per site.

In future works, it would be interesting to determine the conditions for this assumption to be valid, and whether these conditions can be engineered with current technology. Results in this direction would allow excitation schemes to be devised, and also the determination of the control available to tune the density of electrons in the lattice. Also, dynamical calculations aiming at characterizing the lifetime of the lattice configuration after the atoms have been excited to Rydberg levels would allow the evaluation of the time scale available to interrogate the system. The exact calculation of this lifetime is an open problem whose solution is beyond the scope of the present paper. However, the dynamics of our system happens on a time scale of a few hundreds of picoseconds. Techniques for probing electron dynamics on the femtosecond time scale exist in condensed-matter systems (see, e.g., Ref. [50]). These methods might form the basis for resolving the motion of electrons in a Rydberg gas on pico- to femtosecond time scales in future experiments. The use of

---

[1]The SDW susceptibility and the structure factor are defined, respectively, by $\chi(q) = (1/N) \int_0^{1/T} d\tau \Sigma_{i,j} \kappa_i(\tau) \kappa_j(0)$ and $S(q) = (1/N) \Sigma_{i,j} e^{iq(R_i - R_j)} \langle n_i n_j \rangle$, where $\kappa_i(t) = n_{i\uparrow}(t) - n_{i\downarrow}$ and $n_{i,\sigma} = \hat{c}_{i,\sigma}^\dagger \hat{c}_{i,\sigma}$.

our scheme for the purpose of quantum simulation requires the lifetime of the lattice configuration to be longer than the typical time scales of the dynamics. As mentioned by Mourachko *et al.* in Ref. [51], the interatomic spacing (~micrometers) between Rydberg atoms in a frozen gas varies very little (~3%) over a period of time of the order of 1 $\mu$s, some three orders of magnitude larger than the typical hopping times present in the system we have proposed. Also, as already mentioned by Li *et al.* in Ref. [52], fixing the initial positions of the atoms will help to reduce the motion of the ion cores. We therefore believe that Rydberg gases created from ultracold atoms in an optical lattice provide a promising route toward the direct quantum simulation of interacting Fermi systems.

**APPENDIX: REPLACEMENT RULES FOR THE EVALUATION OF TWO-CENTER MOLECULAR INTEGRALS WITH $m=0$**

Here we outline the methods we have used to solve molecular integrals using symbolic replacements. We also provide all the necessary relations to implement the method for $m=0$.

The first step toward the evaluation of these integrals is to express the Coulomb potential in terms of a series of Legendre functions as

$$\frac{1}{r_{12}} = \sum_{k=0}^{\infty} \sum_{m=-k}^{k} \frac{(k-|m|)!}{(k+|m|)!} \frac{r(a)^k}{r(b)^{k+1}} \times P_k^{|m|}(\cos\theta_1) P_k^{|m|}(\cos\theta_2) e^{im(\phi_1-\phi_2)}, \quad \text{(A1)}$$

where $r_{12}$ is the distance between two points with spherical coordinates $(r_i, \theta_i, \phi_i)$, $P_k^{|m|}(x)$ are the associated Legendre functions [we use the notation $P_k^0(x) = P_k(x)$], and $r(a)$, $r(b)$ are the smaller and larger of the quantities $r_1$ and $r_2$; or using the von Neumann expansion

$$\frac{1}{r_{12}} = \frac{2}{R} \sum_{k=0}^{\infty} \sum_{m=-k}^{k} (-1)^m (2k+1) \left(\frac{(k-|m|)!}{(k+|m|)!}\right)^2 P_k^{|m|}[\lambda(a)] Q_k^{|m|} \times [\lambda(b)] P_k^{|m|}(\mu_1) P_k^{|m|}(\mu_2) e^{im(\phi_1-\phi_2)}, \quad \text{(A2)}$$

where in this case the two points are expressed in elliptical coordinates $(\lambda_i, \mu_i, \phi_i)$, $Q_k^{|m|}(x)$ are associated Legendre functions of the second kind, and $\lambda(a)$ is the lesser and $\lambda(b)$ the greater of $\lambda_1$ and $\lambda_2$ (see, e.g., Ref. [19]).

Since the integral $\int_0^{2\pi} e^{i\nu\phi} d\phi$ vanishes if $\nu$ is an integer different from zero, setting the quantum number $m=0$ considerably simplifies the evaluation of the integrals (4) and (5) using the relations (A1) and (A2).

Every two-center molecular integral apart from $W_{\mathbf{p},\mathbf{p}'}^{\mathbf{q},\mathbf{q}'}$ can be evaluated using Eq. (A1). The angular part of these integrals will be nonzero for only a few terms; for instance, for $\mathbf{q}=\mathbf{q}'=(n,0,0)$, the angular part is nonzero for $k=0$, and for $\mathbf{q}=\mathbf{q}'=(n,1,0)$ for $k=0,2$. It may be simplified by using the formula for the product of surface harmonics:

$$P_{\ell_1}(\cos\theta) P_{\ell_2}(\cos\theta) = \sum_{j=|\ell_1-\ell_2|}^{\ell_1+\ell_2} (C_j^{\ell_1,\ell_2})^2 P_j(\cos\theta), \quad \text{(A3)}$$

where $C_j^{\ell_1,\ell_2} = C(\ell_1, \ell_2, j; 0, 0, 0)$ are Clebsch-Gordan coefficients [31]. The integration of the radial part over the coordinates of the first electron necessitates the evaluation of integrals of the form

$$\int_0^{\infty} dr_1 r_1^2 \frac{r(a)^k}{r(b)^{k+1}} a_{\mathbf{q}}(r_1) a_{\mathbf{q}'}(r_1) = I_{\mathbf{q}\mathbf{q}',k}^+(r_2) + I_{\mathbf{q}\mathbf{q}',k}^-(r_2), \quad \text{(A4)}$$

where $a_{\mathbf{q}}(r)$ is the radial part of the wave function (3), and $r_i$ is the coordinate of the $i$th electron. The functionals $I_{\mathbf{q}\mathbf{q}',k}^{\pm}(r_2)$ are defined as

$$I_{\mathbf{q}\mathbf{q}',k}^-(r_2) = (1/r_2^{k+1}) \int_0^{r_2} dr_1 r_1^2 r_1^k a_{\mathbf{q}}(r_1) a_{\mathbf{q}'}(r_1) \quad \text{(A5)}$$

and

$$I_{\mathbf{q}\mathbf{q}',k}^+(r_2) = r_2^k \int_{r_2}^{\infty} dr_1 r_1^2 r_1^{-k-1} a_{\mathbf{q}}(r_1) a_{\mathbf{q}'}(r_1). \quad \text{(A6)}$$

For $k=0$ both (A5) and (A6) can be solved using the rules

$$R3: \quad \int_0^r dr \, e^{-ar} r^k \rightarrow [k! - \Gamma_{k+1}(ar)]/a^{k+1},$$

$$R4: \quad \int_r^{\infty} dr \, e^{-ar} r^k \rightarrow \Gamma_{k+1}(ar)/a^{k+1}. \quad \text{(A7)}$$

If the sum of Eq. (A1) contains only $k=0$ terms, the symbolic form of the integral is obtained by replacing the spherical coordinates of the remaining electron by elliptical coordinates and using the replacement rules of Eqs. (A7) and Table I. In integrals requiring terms associated with $k>0$ in the sum (A1), the functionals associated with $k=0$ dominate [36]. For higher values of $k$, the functional (A6) can always be solved, and as an approximation we have dropped the terms in (A5) that could not be solved analytically using the integration rules mentioned above.

Because it involves associated Legendre functions of the second kind, the evaluation of $W_{\mathbf{p},\mathbf{p}'}^{\mathbf{q},\mathbf{q}'}$ is more problematic. We used the Rodrigues formula to expand these functions in terms of sums of Legendre polynomials and logarithms, and then solved the polynomial part by applying the replacement rules mentioned above. Solving the logarithmic part requires the integration over $\ln(1 \pm x)$ for the first set of coordinates, and then exponential integral functions for the second set.

[1] J. M. Hutson and P. Soldan, Int. Rev. Phys. Chem. **25**, 497 (2006).

[2] G. Thalhammer, K. Winkler, F. Lang, S. Schmid, R. Grimm, and J. H. Denschlag, Phys. Rev. Lett. **96**, 050402 (2006).

[3] B. Knuffman and G. Raithel, Phys. Rev. A **75**, 053401 (2007).

[4] D. DeMille, Phys. Rev. Lett. **88**, 067901 (2002).

[5] C. H. Greene, A. S. Dickinson, and H. R. Sadeghpour, Phys. Rev. Lett. **85**, 2458 (2000).

[6] A. A. Khuskivadze, M. I. Chibisov, and I. I. Fabrikant, Phys. Rev. A **66**, 042709 (2002).

[7] S. M. Farooqi *et al.*, Phys. Rev. Lett. **91**, 183002 (2003).

[8] C. Boisseau, I. Simbotin, and R. Côté, Phys. Rev. Lett. **88**, 133004 (2002).

[9] J. Stanojevic *et al.*, e-print arXiv:0801.2386v1.

[10] T. Gericke *et al.*, e-print arXiv:0804.4788.

[11] R. Saers *et al.*, Eur. Phys. J.: Appl. Phys. **42**, 269 (2008).

[12] K. I. Petsas, A. B. Coates, and G. Grynberg, Phys. Rev. A **50**, 5173 (1994).

[13] M. Lewenstein *et al.*, Adv. Phys. **56**, 243 (2007).

[14] M. Köhl and T. Esslinger, Europhys. News **37**, 18 (2006).

[15] Z. Idziaszek, L. Santos, and M. Lewenstein, Phys. Rev. A **64**, 051402(R) (2001).

[16] T. Cubel, B. K. Teo, V. S. Malinovsky, J. R. Guest, A. Reinhard, B. Knuffman, P. R. Berman, and G. Raithel, Phys. Rev. A **72**, 023405 (2005).

[17] J. Sebby-Strabley, M. Anderlini, P. S. Jessen, and J. V. Porto, Phys. Rev. A **73**, 033605 (2006).

[18] P. W. Atkins and R. S. Friedman, *Molecular Quantum Mechanics* (Oxford University Press, Oxford, 2005).

[19] J. C. Slater, *Quantum Theory of Molecules and Solids* (McGraw-Hill, New-York, 1974), Vol. 1.

[20] J. Stanojevic *et al.*, Eur. Phys. J. D **40**, 3 (2006).

[21] C. A. Coulson, *Valence* (Oxford University Press, Oxford, 1952).

[22] W. Li, I. Mourachko, M. W. Noel, and T. F. Gallagher, Phys. Rev. A **67**, 052502 (2003).

[23] A. V. Stolyarov and M. S. Child, J. Phys. B **32**, 527 (1999).

[24] B. G. Wilson, C. Iglesias, and F. Rogers, Phys. Rev. A **38**, 4633 (1988).

[25] M. Marinescu and A. Dalgarno, Phys. Rev. A **52**, 311 (1995).

[26] M. Marinescu, Phys. Rev. A **56**, 4764 (1997).

[27] R. J. Buehler and J. O. Hirschfelder, Phys. Rev. **83**, 628 (1951).

[28] M. P. Barnett, Int. J. Quantum Chem. **95**, 791 (2003).

[29] J. Fernández Rico, R. López, G. Ramírez, and C. Tablero, Phys. Rev. A **49**, 3381 (1994).

[30] M. P. Barnett, J. Symb. Comput. **42**, 265 (2007).

[31] M. P. Barnett, J. Chem. Phys. **113**, 9419 (2000).

[32] D. Jaksch, C. Bruder, J. I. Cirac, C. W. Gardiner, and P. Zoller, Phys. Rev. Lett. **81**, 3108 (1998).

[33] T. F. Gallagher, *Rydberg Atoms* (Cambridge University Press, Cambridge, U.K., 1994).

[34] E. Toth, A. M. Rey, and P. B. Blakie, e-print arXiv:08032922.

[35] M. Köhn and T. Esslinger, Europhys. News **37**, 18 (2005).

[36] J. Appel, M. Grodzicki, and F. Paulsen, Phys. Rev. B **47**, 2812 (1993).

[37] N. W. Ashcroft and N. D. Mermin, *Solid State Physics* (W. B. Saunders/Brooks–Cole Thomson Learning, Philadelphia, 1976).

[38] A. Painelli and A. Girlando, Phys. Rev. B **39**, 2830 (1989).

[39] F. Marsiglio and J. E. Hirsch, Phys. Rev. B **41**, 6435 (1990).

[40] J. T. Gammel and D. K. Campbell, Phys. Rev. Lett. **60**, 71 (1988).

[41] D. Baeriswyl, P. Horsch, and K. Maki, Phys. Rev. Lett. **60**, 70 (1988).

[42] S. Trotzky *et al.*, Science **319**, 295 (2008).

[43] A. M. Rey, P. B. Blakie, G. Pupillo, C. J. Williams, and C. W. Clark, Phys. Rev. A **72**, 023407 (2005).

[44] E. Kaxiras, *Atomic and Electronic Structure of Solids* (Cambridge University Press, Cambridge, U.K., 2002).

[45] I. S. Elfimov, S. Yunoki, and G. A. Sawatzky, Phys. Rev. Lett. **89**, 216403 (2002).

[46] J. E. Hirsch, Phys. Rev. B **48**, 9815 (1993).

[47] D. Duffy and A. Moreo, Phys. Rev. B **52**, 15607 (1995).

[48] M. Raczkowski, R. Frésard, and A. M. Oles, Europhys. Lett. **76**, 128 (2006).

[49] S. Sachdev and S.-C. Zhang, Science **295**, 452 (2002).

[50] A. Cavalleri, M. Rini, H. H. W. Chong, S. Fourmaux, T. E. Glover, P. A. Heimann, J. C. Keiffer, and R. W. Schoenlein, Phys. Rev. Lett. **95**, 067405 (2005).

[51] I. Mourachko, W. Li, T. F. Gallagher, Phys. Rev. A **70**, 031401(R) (2004).

[52] W. Li, P. J. Tanner, and T. F. Gallagher, Phys. Rev. Lett. **94**, 173001 (2005).